

---

# GaussianDreamerPro: Text to Manipulable 3D Gaussians with Highly Enhanced Quality

---

Taoran Yi<sup>1</sup>, Jiemin Fang<sup>2†</sup>, Zanwei Zhou<sup>3</sup>, Junjie Wang<sup>2</sup>, Guanjun Wu<sup>4</sup>,  
Lingxi Xie<sup>2</sup>, Xiaopeng Zhang<sup>2</sup>, Wenyu Liu<sup>1‡</sup>, Xinggong Wang<sup>1†</sup>, Qi Tian<sup>2</sup>

<sup>1</sup>School of EIC, Huazhong University of Science and Technology <sup>2</sup>Huawei Inc.

<sup>3</sup>MoE Key Lab of Artificial Intelligence, AI Institute, Shanghai Jiao Tong University

<sup>4</sup>School of CS, Huazhong University of Science and Technology

{taoranyi, guajuwu, liuwu, xgwang}@hust.edu.cn

{jaminfang, is.wangjunjie, 198808xc, zxphistory}@gmail.com

SJTU19zzw@sjtu.edu.cn tian.qil@huawei.com

## Abstract

Recently, 3D Gaussian splatting (3D-GS) has achieved great success in reconstructing and rendering real-world scenes. To transfer the high rendering quality to generation tasks, a series of research works attempt to generate 3D-Gaussian assets from text. However, the generated assets have not achieved the same quality as those in reconstruction tasks. We observe that Gaussians tend to grow without control as the generation process may cause indeterminacy. Aiming at highly enhancing the generation quality, we propose a novel framework named GaussianDreamerPro. The main idea is to bind Gaussians to reasonable geometry, which evolves over the whole generation process. Along different stages of our framework, both the geometry and appearance can be enriched progressively. The final output asset is constructed with 3D Gaussians bound to mesh, which shows significantly enhanced details and quality compared with previous methods. Notably, the generated asset can also be seamlessly integrated into downstream manipulation pipelines, *e.g.* animation, composition, and simulation *etc.*, greatly promoting its potential in wide applications. Demos are available at <https://taoranyi.com/gaussiandreamerpro/>.

## 1 Introduction

The past year has witnessed great success and rapid development of 3D Gaussian splatting (3D-GS) [2] in 3D reconstruction and rendering. 3D-GS shows highly realistic rendering effects while enjoying notably fast rendering and training. It has become a popular 3D representation and carries great potential to be applied to various tasks.

3D generation from text [1, 3–9] is one of the most appealing tasks where researchers have made great efforts to generate high-quality 3D assets, which may benefit the industry of game, movie, and XR *etc.* Many recent works [1, 10–14] expect to transfer the high rendering quality of 3D-GS to the generation task and have made a series of explorations. Though some good 3D assets based on Gaussians can be obtained, the quality still cannot meet the requirements for real applications. *E.g.*, the detail generation is limited and the surfaces of 3D assets are usually blurred as shown in Fig. 2. We delve into the problem and analyze the key reasons as follows. Different from the reconstruction task which is based on deterministic information, *e.g.* captured images or videos, the generation

---

<sup>†</sup>Project lead.

<sup>‡</sup>Corresponding author.



Figure 1: GaussianDreamerPro can generate high-quality 3D assets based on text and can be applied to downstream manipulation pipelines.

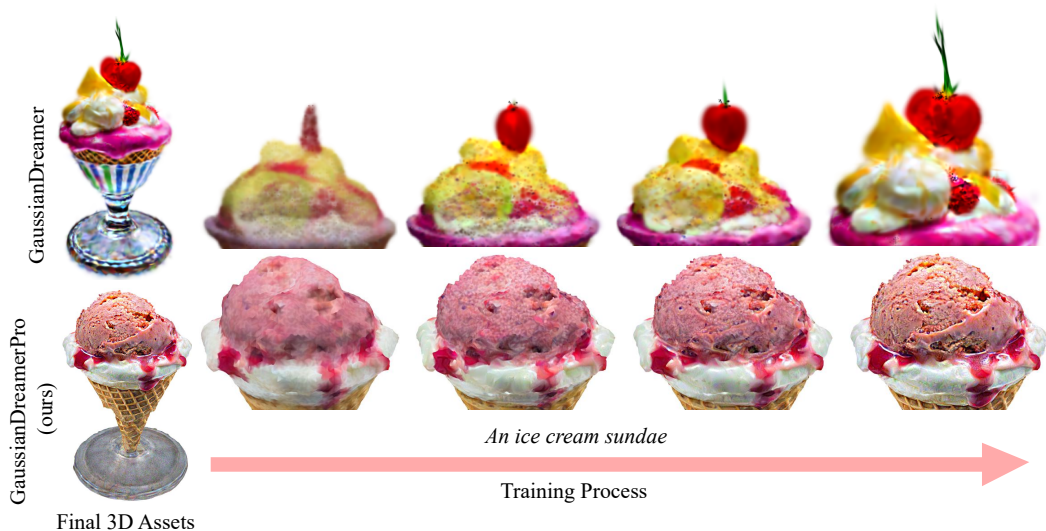


Figure 2: We show the changes in 3D assets during the training process of GaussianDreamer [1] and our method. Compared with GaussianDreamer, which grows Gaussians uncontrollably, resulting in always blurry edges, our method continuously improves the quality of appearance under the constraint of geometry.

task faces more indeterminacy as one text prompt may correlate to various samples with different characters. During the optimization process, 3D Gaussians tend to grow without control towards various directions. This makes it hard to reach a stable state which largely limits the enrichment of details and results in blurred surfaces and appearance.

To tackle the above challenge, we propose a novel text-to-3D generation framework, named GaussianDreamerPro, aiming at largely enhancing the quality and details of generated 3D-Gaussian assets. The main idea is to bind Gaussians to reasonable geometry which can constrain Gaussians in growing or changing in a controllable range. To make the final generated asset own enough details, we propose to progressively enrich the geometry over 3 stages of generation. Inherited from the basic framework of GaussianDreamer [1], we first obtain an initial 3D asset with extremely coarse geometry and appearance from the 3D diffusion model, *e.g.* Shap-E [15]. Then we transform the initial asset into a set of 2D Gaussians which can better align the surface and are optimized using the 2D diffusion model. Here we obtain a basic 3D asset whose appearance and geometry are improved to basically meet the requirements. Subsequently, we export a mesh structure with colored vertices from the 2D Gaussians. A series of 3D Gaussians are initialized and bound to the exported mesh. The geometry-bound 3D Gaussians are finally optimized to get the final asset with details highly-enhanced. The asset geometry is progressively evolving through the overall pipeline. Simultaneously, due to the geometry constrain, the appearance can also be enriched continually. Besides, as the final asset is constructed as 3D Gaussians with mesh bound, it can be seamlessly integrated to downstream manipulation pipelines, *e.g.* animation, combination, and simulation *etc.*

Our contributions can be summarized as follows.

- We design a novel text-to-3D-Gaussians generation framework, which optimize Gaussians with geometry guided, resulting in both the geometry and appearance evolve progressively.
- The proposed method can generate 3D assets with quality significantly enhanced compared with previous works.
- The generated assets can be seamlessly integrated into downstream manipulation applications.
- The framework is compatible with other 3D generation methods, *e.g.* further enhancing 3D assets generated by DreamCraft3D [7].

## 2 Related Work

**Text to 3D Generative Models.** Recently, text-to-3D generative models [16–19, 4–9] have made significant progress, achieving high quality in generating both 3D objects and 3D scenes. Some methods [20–27] align the 2D images rendered from 3D representations and text with CLIP [28], thereby generating 3D objects or scenes that match the text description. Currently, there are also some methods [11, 10, 3, 19, 29, 4, 5, 26, 9, 8, 30] that lift 2D diffusion models [31–33] to 3D. Specifically, they bring the distribution of images rendered from 3D representations closer to the distribution of images generated by 2D diffusion models under text conditions through gradient descent, thereby optimizing to obtain 3D representations that meet text conditions. For example, DreamFusion [3] and [29] have proposed the Score Distillation Sampling (SDS) and Score Jacobian Chaining (SJC) methods based on this, respectively. This method can achieve good results in generating 3D objects and 3D scenes from text. And because diffusion has a stronger understanding of the text, it can achieve better generation results compared to using CLIP. Some methods [34–47] use 2D diffusion models fine-tuned with camera pose as a condition to achieve 3D generation from a single image. In addition, there are also some methods [15, 48–52, 13, 14, 53] that generate 3D objects only by inference, by pretraining on 3D data and text pairs, to achieve the effect of directly generating 3D objects from text, which is often much shorter in time than the method of lifting 2D diffusion models to 3D. However, compared to the method of lifting 2D diffusion models to 3D, the training cost of 3D data and text pairs is higher.

**3D Representation Methods.** Recently, Neural Radiance Fields (NeRF) [54] have achieved great success in representing 3D scenes, achieving realistic and reliable rendering quality. Some variants [55–60] use explicit representation to greatly increase the optimization speed, compensating for the optimization speed issue of NeRF. There are also some methods [61, 62] that further improve the quality of NeRF. Many methods apply NeRF and its variants to the field of 3D generation, achieving high-quality results. In addition, Magic3D [19], Fantasia3D [4], *etc.*, introduce the explicit

optimizable representation DMTET [31] into 3D generation, achieving higher quality than using NeRF due to its geometry constraints. Recently, 3D Gaussian Splatting (3D-GS) [2], as a new 3D representation method, has further accelerated the rendering speed and quality. Some variants of 3D Gaussian Splatting [63–65] improve the geometry and rendering quality. After introducing 3D Gaussians in the field of 3D generation, the 3D generation based on 3D Gaussian Splatting can achieve real-time rendering speed while having high-quality rendering effects. DreamGaussian [11] uses 3D Gaussians as the optimized 3D representation, further exported as a mesh with optimized texture. GaussianDreamer [1] and GSGEN [10] use the characteristics of 3D Gaussians to apply 2D and 3D diffusion models together in the 3D generation process. There are methods [64, 66–70] that combine mesh and 3D Gaussians as 3D representation. This representation can be combined with traditional graphics pipelines, making it more versatile. One concurrent work [71] uses this representation method to generate 3D assets, taking advantage of its geometry prior.

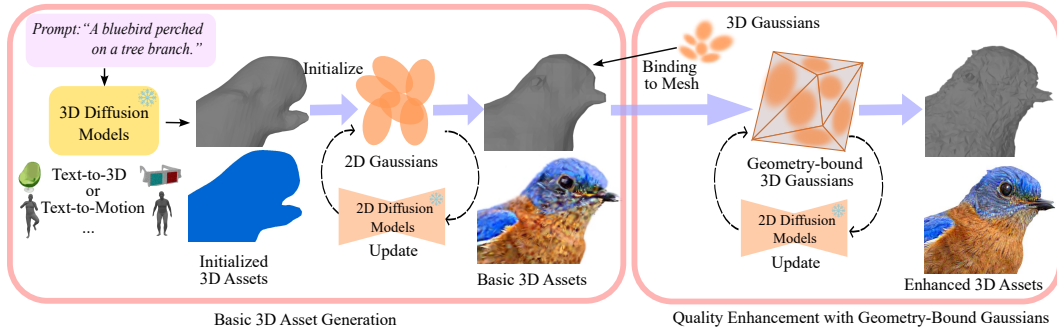


Figure 3: Our framework can be divided into two parts: basic 3D asset generation and quality enhancement with geometry-bound Gaussians. In the basic 3D asset generation stage, we generate initial 3D assets, which are used to initialize 2D Gaussians, obtain basic 3D assets under the optimization of the 2D diffusion model, and export as a mesh. In the quality enhancement with geometry-bound Gaussians stage, we bind 3D Gaussians to the mesh, and also obtain enhanced 3D assets under the optimization of the 2D diffusion model.

### 3 Method

In this section, we first review the 3D Gaussian splatting [2] and 3D generation model. In Sec. 3.2, we provide an overview of the whole framework. Then in Sec. 3.3 and Sec. 3.4, we elaborate on the processes of the two stages of generating basic geometry and highly-detailed texturing with 3D Gaussians, respectively.

#### 3.1 Preliminaries

**3D Gaussian Splatting.** 3D Gaussian Splatting [2] is a novel method for representing 3D scenes, achieving excellent rendering quality. It uses a series of 3D Gaussians to represent the scene, each 3D Gaussian contains its center position  $\mu_o \in \mathbb{R}^3$ , color  $c_o \in \mathbb{R}^3$ , opacity  $o_o \in \mathbb{R}^1$ , and covariance  $\Sigma_o$ . For ease of optimization, the covariance matrix is decomposed into a vector  $s_o \in \mathbb{R}^3$  for scaling and a quaternion  $q_o \in \mathbb{R}^4$  to represent rotation. Therefore we can represent the 3D Gaussians  $\theta_o$  as:

$$\theta_o = (\mu_o, c_o, o_o, \Sigma_o = (s_o, q_o)) \quad (1)$$

When computing the color  $C(r)$  of the corresponding pixel rendered by the ray  $r$ , 3D Gaussians are splatted into the 2D pixel space. The computation is as follows:

$$C(r) = \sum_{i \in \mathcal{N}} c_i \alpha_i \prod_{j=1}^{i-1} (1 - \alpha_j), \quad \alpha_i = o_i G(x_i), \quad G(x_i) = e^{-\frac{1}{2} x_i^T \Sigma_i^{-1} x_i}, \quad (2)$$

where  $\mathcal{N}$  is the number of 3D Gaussians along the ray  $r$  and  $c_i$  represent the color of the  $i$ -th 3D Gaussian,  $x_i$  is the offset between the center of the splatted Gaussian and the pixel.  $G$  stands for 3D Gaussians' spatial distribution. In 3D Gaussians, the depth of a certain Gaussian in a ray is usually approximated by the depth of its center, which leads to an inaccurate surface.

**3D Generation Methods.** Thanks to the Gaussian Splatting [2] representation based on 3D points, GaussianDreamer [1] can be optimized under the geometry guidance provided by the 3D diffusion model. With the geometry guidance provided by the 3D diffusion model, the generated 3D assets have better 3D consistency. Then the details of 3D Gaussians are further enriched with the 2D diffusion model. Finally, the generated 3D assets have good 3D consistency provided by the 3D diffusion model and fine details from the 2D diffusion model. When enriching the details of 3D Gaussians using the 2D diffusion model  $\phi$ , GaussianDreamer adopts the SDS loss proposed by DreamFusion [3]. In the SDS loss, the 3D representation  $\theta$  first renders the image  $\mathbf{x} = g(\theta)$  from a given camera pose, where  $g$  denotes the differentiable rendering process. Then a random noise  $\epsilon$  is added to  $\mathbf{x}$  to produce the noisy image  $\mathbf{x}_t$ . DreamFusion uses a scoring estimation function  $\hat{\epsilon}_\phi(\mathbf{x}_t; y, t)$  to predict the sampled noise based on the given noisy image  $\mathbf{x}_t$ , text condition  $y$ , and noise level  $t$ . The difference between the predicted noise  $\hat{\epsilon}_\phi$  and the added random noise  $\epsilon$  provides the direction for gradient update:

$$\nabla_\theta \mathcal{L}_{\text{SDS}}(\phi, \mathbf{x} = g(\theta)) \triangleq \mathbb{E}_{t, \epsilon} [w(t) (\hat{\epsilon}_\phi(\mathbf{x}_t; y, t) - \epsilon) \frac{\partial \mathbf{x}}{\partial \theta}], \quad (3)$$

where  $w(t)$  is a weighting function. LucidDreamer [12] proposes a multi-step iterative method to predict noise and introduces the (Interval Score Matching) ISM loss, reducing the difficulty of prediction. LucidDreamer first obtains the predicted noise  $\hat{\epsilon}_\phi(\mathbf{x}_s; \emptyset, s)$  at noise level  $s = t - \delta_T$ , where  $\delta_T$  is the Denoising Diffusion Implicit Model (DDIM) [72] inversion step size and  $\emptyset$  represents the empty text prompt. Then, through DDIM inversion,  $\mathbf{x}_t$  is obtained. Compared to Eq. 3, the gradient of ISM loss is modified as

$$\nabla_\theta \mathcal{L}_{\text{ISM}}(\phi, \mathbf{x} = g(\theta)) \triangleq \mathbb{E}_{t, \epsilon} [w(t) \underbrace{(\hat{\epsilon}_\phi(\mathbf{x}_t; y, t) - \hat{\epsilon}_\phi(\mathbf{x}_s; \emptyset, s))}_{\text{ISM update direction}} \frac{\partial \mathbf{x}}{\partial \theta}]. \quad (4)$$

### 3.2 Overall Framework

Our method, as illustrated in Fig. 3, is divided into two stages: **basic 3D assets generation and quality enhancement with geometry-bound Gaussians**. In the **basic 3D assets generation** stage, We use 2D Gaussians [63] as our 3D representation method, which allows us to obtain a more accurate surface while benefiting from the geometry guidance of the 3D diffusion model. We first use a 3D diffusion model to generate a mesh  $M_i$  under a text condition  $y$ , which serves as the initialization for the 2D Gaussians  $\theta_g$ . Subsequently, we utilize a text-to-image 2D diffusion model  $\phi$  to optimize the 2D Gaussians  $\theta_g$  based on the text condition  $y$ . After the optimization, our 3D representation method exports the 2D Gaussians  $\theta_g$  as the basic geometry mesh  $M_b$ . In the **quality enhancement with geometry-bound Gaussians** stage, we first construct a series of 3D Gaussians  $\theta_r$ , then bind the 3D Gaussians to the surface of the basic geometry mesh  $M_b$ . Through the bound 3D Gaussians, we expect high-quality rendering effects while having a more precise geometric structure. We also leverage the text-to-image 2D diffusion model  $\phi$  to optimize the 3D Gaussians, binding the 3D Gaussians  $\theta_r$  on the surface of the basic geometry mesh  $M_b$  during the optimization process. In the end, we obtain optimized 3D assets based on the 3D Gaussian representation. Throughout this process, from the initialize mesh  $M_i$  to the basic geometry mesh  $M_b$  exported from the 2D Gaussians  $\theta_g$ , and finally to the 3D assets represented by 3D Gaussians  $\theta_r$ , the geometry evolves continuously. Based on this continuously evolving geometry, we achieve 3D assets with progressively improving quality. By binding the 3D Gaussians on the mesh, we can integrate the generated assets into traditional graphics pipelines, making our method applicable to animation and simulation.

### 3.3 Basic 3D Asset Generation

3D Gaussian Splatting [2] and their variants serve as explicit representation methods that can effectively utilize the coarse geometry generated by 3D diffusion models. However, due to the multi-view inconsistency of 3D Gaussian distributions, 3D Gaussians cannot accurately represent surfaces, resulting in generated 3D assets with rough and imprecise geometry. Inspired by 2D Gaussian Splatting [63], we flatten the original 3D Gaussians of the ellipse into a 2D surfel to accurately model the geometry of the 3D assets. Different from 3D Gaussians in Eq. 1, the scale vector  $s_g$  is represented as  $s_g = (s_u, s_v) \in \mathbb{R}^2$ , which controls the variances of the 2D Gaussians. Therefore, the 3D representation to be optimized is denoted as  $\theta_g(\mu_g, c_g, o_g, s_g, q_g)$ , where  $\mu_g$  is the position of the center,  $c_g$  is the color, and  $o_g$  is the opacity. Its rendering process is similar to Eq. 2. This representation allows us to leverage the coarse geometry guidance generated by 3D diffusion

models while enjoying the precise surface of 3D assets. Specifically, we first use the 3D diffusion model Shap-E [15] to obtain an initialized mesh  $M_i$ . Then, we use the mesh  $M_i$  to initialize the 2D Gaussians  $\theta_g$ . The center coordinates  $\mu_g$  of 2D Gaussians are obtained from vertices of the mesh  $M_i$  vertices as initialization. With the geometry guidance of the 3D diffusion model, 2D Gaussians can start from a geometry with good 3D consistency, greatly avoiding the multi-face problem. Based on the text condition  $y$  and given camera poses, we render the image  $\mathbf{x}$ , randomly give the noise level  $s$ , get noised images  $\mathbf{x}_s$  in Eq. 4, and get  $\mathbf{x}_t$  based on the DDIM inversion process described in Sec. 3.1. Through Eq. 4, with the text  $y$  and the text-to-image diffusion model  $\phi$ , we can obtain the direction for updating our 3D representation. Finally, we perform Poisson reconstruction [73] based on the center position  $\mu_g$  of the 2D Gaussians  $\theta_g$ , exporting the 2D Gaussians  $\theta_g$  as a mesh  $M_b$ .  $v_m$  and  $c_m$  denote the vertices of the mesh  $M_b$  and the colors of the mesh vertices, respectively. The color  $c_m$  is obtained from the color  $c_g$  of the Gaussians around the vertices  $v_m$ . The obtained mesh is represented as follows:

$$M_b = (v_m \in \mathbb{R}^{V \times 3}, c_m \in \mathbb{R}^{V \times 3}, t_m = (v_m^1, v_m^2, v_m^3) \in \mathbb{R}^{V \times 3 \times 3}), v_m \leftarrow \mu_g, c_m \leftarrow c_g, \quad (5)$$

where  $V$  denotes the number of triangles in the mesh  $M_b$ .  $v_m^1, v_m^2, v_m^3$  represent the coordinates of the three vertices that form the triangle  $t_m$  of the mesh  $M_b$ . Compared to the elliptical geometry of 3D Gaussians, the surfel geometry of 2D Gaussians greatly reduces the difficulty of calculating level sets, resulting in a better 3D geometry mesh that can be exported.

### 3.4 Quality Enhancement with Geometry-Bound Gaussians

**Binding Gaussians to Mesh** In the previous stage, we obtained the basic geometry – mesh  $M_b$ . We bind 3D Gaussians on  $M_b$  to get high-quality 3D assets. Compared to optimizing texture maps, we hope that optimizing the bound 3D Gaussians can achieve better rendering effects. We first construct  $V$  clusters of 3D Gaussians  $\theta_r$ , which is the same as the number of triangles in the mesh  $M_b$ , and each cluster contains  $N$  3D Gaussians. With the help of Eq. 1, we denote the 3D Gaussians as:

$$\begin{aligned} \theta_r &= (\theta_{r1}, \theta_{r2}, \dots, \theta_{ri}, \dots, \theta_{rV}), \\ \theta_{ri} &= (\mu_{ri} \in \mathbb{R}^{N \times 3}, c_{ri} \in \mathbb{R}^{N \times 3}, \alpha_{ri} \in \mathbb{R}^N, q_{ri} \in \mathbb{R}^{N \times 4}, s_{ri} \in \mathbb{R}^{N \times 3}). \end{aligned} \quad (6)$$

Here,  $i$  represents the  $i$ -th cluster of 3D Gaussians  $\theta_r$ . Following Sugar [64], we use frozen barycentric weight  $W_b = (W_{b1}, W_{b2}, W_{b3}) \in \mathbb{R}^{N \times 3}$  and the mesh vertices  $v_m$  to calculate the position  $\mu_{ri}$  of each Gaussian in the mesh triangle  $t_m = (v_m^1, v_m^2, v_m^3)$ , binding the Gaussian in the triangle. The calculation process is as follows:

$$\mu_{ri} = W_{b1} * v_m^1[i] + W_{b2} * v_m^2[i] + W_{b3} * v_m^3[i]. \quad (7)$$

When the colors  $c_{ri}$  of each Gaussian are initializing, it is similar to Eq. 7, using the colors  $c_m$  of the mesh and  $W_b$  to calculate. This ensures that the Gaussians are evenly distributed within the triangle, as can be seen in Fig. 3.

**Optimizing Gaussians with Geometry Constraints** Since  $W_b$  here is frozen, 3D Gaussians are tightly bound to the mesh. Rather than directly optimizing the position of each Gaussian, we optimize the coordinates  $v_m$  of the mesh vertices. However, the colors  $c_{ri}$  of each Gaussian will be directly optimized. In order to ensure the alignment with the mesh triangle, the rotation of the Gaussian becomes 2D rotation  $q_{ri} \in \mathbb{R}^{N \times 2}$ . We maintain the scales  $s_{ri}$  in 3D learnable, which ensures that the texture of the mesh surface is more realistic. Similar to the previous stage, we also use Eq. 4 to optimize our 3D representation, further improving the details of the representation, and obtain 3D assets with 3D Gaussians as textures bound onto the mesh. In the optimization process, our geometry evolves once again, highlighting the details on the surface.

**Asset Manipulation** The position  $\mu_{ri}$  of the 3D Gaussian is connected with the mesh vertices  $v_m$  using barycentric weights  $W_b$ . Therefore, when the mesh vertices  $v_m$  are changed to  $\hat{v}_m$  through the traditional graphics pipeline, such as physical animation, simulation, *etc.* [70, 69], we can calculate the center coordinates  $\hat{\mu}_{ri}$  of the 3D Gaussians  $\hat{\theta}_{ri}$  following the mesh changes through the barycentric weight  $W_b$ , according to Eq. 7. Finally, through Eq. 2, we can get the rendered image of changed 3D Gaussians.



Figure 4: Qualitative comparisons between our method and LucidDreamer [12], DreamCraft3D [7], DreamFusion [3], Magic3D [19], Fantasia3D [4], GaussianDreamer [1] and GSGEN [10].



Figure 5: Animation and simulation of the generated 3D assets.

## 4 Experiments

In this section, we elaborate on the implementation details in Sec. 4.1. We show the results of a user study in Sec. 4.2, provide visual results of our method in Sec. 4.3, and conduct ablation experiments on relevant parts in Sec. 4.4. In the final section, we discuss the limitations of our method.

### 4.1 Implementation Details

Our method is implemented in PyTorch [74], using Adam [75] as the optimizer. The 2D text-to-image diffusion model we use is "stabilityai/stable-diffusion-2-1-base"<sup>1</sup> [76], with classifier-free guidance (CFG) size of 7.5. The step size we use is from 0.02 to 0.5. The Shap-E [15] we use loads the model fine-tuned on Objaverse [77] in Cap3D [78]. The batch size used in the two stages of the framework is 4, the resolution of the rendered image is 1024x1024, and it is downsampled to 512x512 when optimizing with the 2d diffusion model. Both are trained for 5000 iterations. When rendering images, the radius of the camera pose used is from 3.5 to 5.5, azimuth is from -180 degrees to 180 degrees, and elevation is from 30-150 degrees. In the basic geometry generation stage, the learning rate of the position of 2D Gaussians is  $1.6 \times 10^{-5}$ , and in the quality enhancement with geometry-bound Gaussians stage, the learning rate of the position of 3D Gaussians is  $1.6 \times 10^{-4}$ . In addition, the learning rates of color and opacity for both types of Gaussians are  $5 \times 10^{-3}$  and  $5 \times 10^{-2}$ , and the learning rates of scale and rotation are both  $5 \times 10^{-4}$ . The entire training process is completed on an RTX V100 32G, and it takes about 3 hours.

### 4.2 User Study

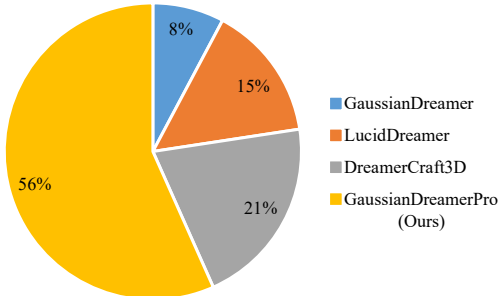


Figure 6: Results of user study.

In order to better evaluate the quality of our method, we conducted a series of user studies using 3D assets generated from 10 prompt words. We separately display videos of 3D assets generated by methods GaussianDreamer [1], LucidDreamer [12], DreamCraft3D [7], and our method with the same text prompt. Each participant watches these videos and make a choice on which 3D asset has higher quality. We collected 270 responses from 27 participants, where the statistics are organized as Fig. 6. Our method wins the favor of 56% of users, and its performance is much better than other methods. This

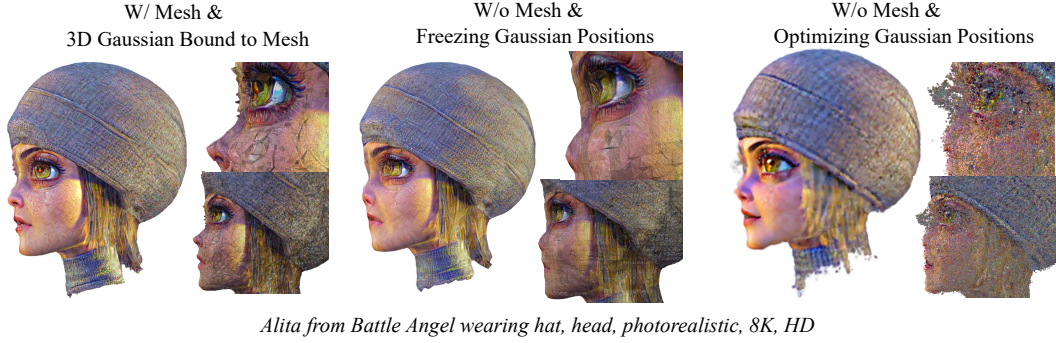
result indicates that the 3D assets we generate have better quality.

### 4.3 Visualization Results

We present the visualization results of the 3D assets generated by our method, and first compare with the two most recent methods for generating 3D assets – LucidDreamer [12] and Dreamcraft3D [7], which are respectively one of the best 3D generative methods based on Gaussian and one of the best 3D generative methods based on optimizable mesh. Dreamcraft3D is different from other methods, it generates 3D assets based on text prompts and a reference image as conditions. Our method is well compatible with the generation method based on optimizable mesh, which we discuss in detail in Sec. 4.4. Our method shows good quality compared to the other two methods, with higher clarity and better geometry compared to LucidDreamer. In the visualization results of Dreamcraft3D [7], we have placed the required reference image in the top right, while the other images are the rendering results of the generated 3D assets from Dreamcraft3D. It can be observed that the viewpoint close to the reference image often achieves good results, but the back of the "croissant" lacks detail. Our method has stronger 3D consistency and does not require reference images. Moreover, we provide comparisons with DreamFusion [3], Magic3D [19], Fantasia3D [4], GaussianDreamer [1], and GSGEN [10], where DreamFusion uses a NeRF-based [54, 61] representation method, Magic3D and Fantasia3D use an optimizable mesh [31] method as the 3D representation method, GaussianDreamer and GSGEN use 3D Gaussians as the representation method, our method shows better geometry

<sup>1</sup><https://huggingface.co/stabilityai/stable-diffusion-2-1-base>





Alita from Battle Angel wearing hat, head, photorealistic, 8K, HD

Figure 7: Ablation experiments on geometry constraints.

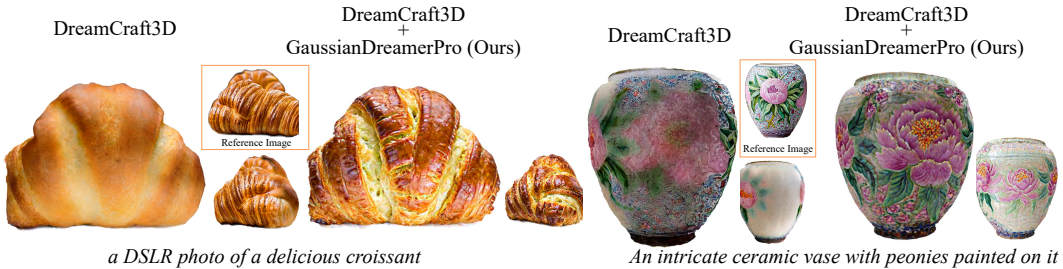


Figure 8: The results of applying our method to DreamCraft3D [7].

and appearance details. Please zoom in Fig. 4 for a better comparison. We also show the results of animation and simulation of our generated 3D assets in Fig. 5.

#### 4.4 Ablation Study and Analysis

In this section, we conduct ablation experiments on the key components of our method to verify the role of key components.

**Geometry-Bound Gaussians.** We show the results of ablating bound geometry in Fig. 7. Each sample’s left image is the rendered image, and the right image is the result of visualizing the point cloud saved by the Gaussian coordinates and colors. We try to find the connection between the Gaussian position and the rendering quality. In the first one, we bind the Gaussians to the mesh to establish good geometry constraints. In the second one, after initializing the Gaussian positions using Eq. 7, we removed the mesh. We fix the position of the Gaussians, and the optimization of other parameters is the same as the first one. Compared to the first one, there are fewer geometry constraints here, but freezing the Gaussian positions can to some extent simulate the previous geometry constraints. Compared to fixing the position of the Gaussians, binding the Gaussians to the mesh surface allows us to optimize the vertices of the mesh to optimize the position of the Gaussians through Eq. 7. Therefore, we can see that the character’s nose and eyes have better quality in the first one. On the last one, we do not add geometry constraints, and directly convert the Gaussians from the basic 3D assets into 3D Gaussians, without the process of geometry-bound, and the other optimization methods are the same. We can see that without geometry constraints, the rendered image is unclear, and we can see that compared to having geometry constraints, there are many discrete Gaussians on the edge and surface of the object, and the position of the Gaussians is very scattered. It is these discrete Gaussians that surround the surface of the object, making the object blurry, and unable to have clear edges and rendering quality. After adding geometry constraints, the growth of Gaussians is controlled, the surface no longer has discrete Gaussians, and clear high-detail images are rendered.

**Compatibility with Dreamcraft3D** In this section, we apply GaussianDreamerPro to Dream-Craft3D [7], demonstrating that our method is also friendly to DreamCraft3D. Our results are shown in Fig. 8. Since the back of the 3D assets generated by DreamCraft3D sometimes suffers from a lack

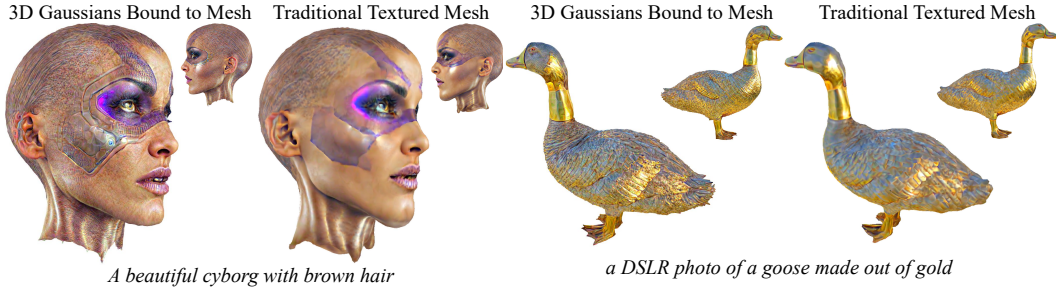


Figure 9: Comparison between enhanced 3D assets optimized with 3D Gaussians bound to mesh and traditional textured mesh.

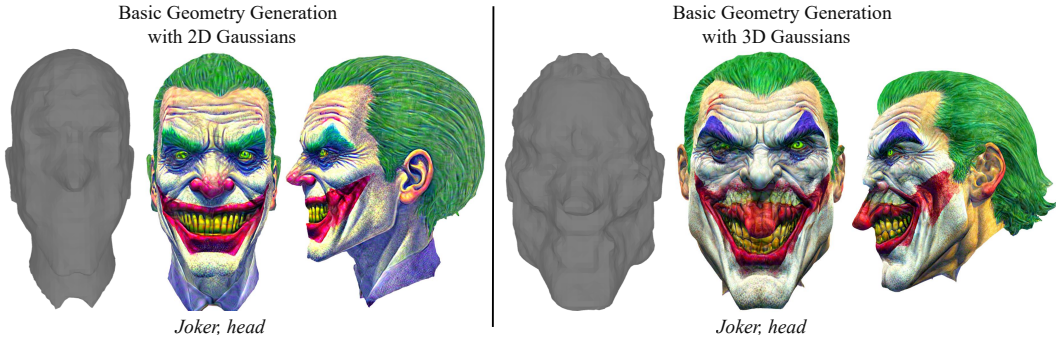


Figure 10: Ablation experiments on the representation method of basic 3D assets.

of detail, we use DreamCraft3D as our basic 3D assets and further adopt the method in Sec. 3.4 for fine-tuning. The results in Fig. 8 show that after fine-tuning, the details on the back of DreamCraft3D can be greatly improved, generating better 3D assets.

**Texturing with 3D Gaussians.** In the quality enhancement with geometry-bound Gaussians stage, we use 3D Gaussians [2] as the texture for generating 3D assets. In this section, we conduct ablation experiments to demonstrate that 3D Gaussians as textures have better rendering effects. As comparisons, we change the optimization target of this stage from 3D Gaussians to traditional textured mesh, and we optimize the same number of iterations. Fig. 9 shows our visualization results. Compared to optimizing textured mesh, 3D Gaussians can display higher quality rendering effects. Thanks to the scale of 3D Gaussians in all three dimensions, the 3D assets generated using 3D Gaussians, such as the feathers of the goose in Fig. 9, have a more realistic texture.

**Using 2D Gaussians for Basic 3D Assets Generation.** In the stage of basic 3D assets generation, we use 2D Gaussians [63] as a 3D representation. In this section, we conduct ablation experiments on this 3D representation, comparing it with the use of 3D Gaussians [2], to verify that it can generate better basic geometry and its impact on the final generation of 3D assets. We present our ablation results in Fig. 10. Compared to the representation method of using 3D Gaussians in the stage of basic 3D assets generation, using 2D Gaussians can generate better geometry. The visualization quality of the final generated 3D assets is higher, and the consistency is better.

#### 4.5 Limitations

Our method can generate high-quality single objects based on text input, but when dealing with combinations of multiple objects, it sometimes only generates one of the objects, such as the boots in Fig. 1. This limitation occurs because the geometry guidance provided by the 3D diffusion model results in the initialized 3D asset. This asset only includes some of the objects described in the prompt when multiple objects are involved. Consequently, these incorrectly initialized 3D assets lead to the incorrectness of final enhanced 3D assets. In future work, it may be possible to achieve better geometry guidance and generate better examples of multiple object combinations by pretraining 3D diffusion models on multiple object dataset.

## 5 Conclusion

In this paper, we propose a novel text-to-3D Gaussian generation framework – GaussianDreamerPro, which significantly enhances the quality compared with previous works. The asset geometry is progressively improved over the generation pipeline. With bound to the geometry, 3D Gaussians can be optimized under constraints in a reasonable range, also resulting in continuously enriched appearance. Moreover, the generated assets can be directly applied to various downstream manipulation pipelines. We also demonstrate the universality of the proposed method by further enhancing the quality of assets generated by DreamCraft3D [7].

## References

- [1] Taoran Yi, Jiemin Fang, Guanjin Wu, Lingxi Xie, Xiaopeng Zhang, Wenyu Liu, Qi Tian, and Xinggang Wang. Gaussiandreamer: Fast generation from text to 3d gaussian splatting with point cloud priors. *arXiv preprint arXiv:2310.08529*, 2023.
- [2] Bernhard Kerbl, Georgios Kopanas, Thomas Leimkühler, and George Drettakis. 3d gaussian splatting for real-time radiance field rendering. *ACM Transactions on Graphics*, 42(4), July 2023.
- [3] Ben Poole, Ajay Jain, Jonathan T Barron, and Ben Mildenhall. Dreamfusion: Text-to-3d using 2d diffusion. *arXiv preprint arXiv:2209.14988*, 2022.
- [4] Rui Chen, Yongwei Chen, Ningxin Jiao, and Kui Jia. Fantasia3d: Disentangling geometry and appearance for high-quality text-to-3d content creation. *arXiv preprint arXiv:2303.13873*, 2023.
- [5] Zhengyi Wang, Cheng Lu, Yikai Wang, Fan Bao, Chongxuan Li, Hang Su, and Jun Zhu. Prolific-dreamer: High-fidelity and diverse text-to-3d generation with variational score distillation. *arXiv preprint arXiv:2305.16213*, 2023.
- [6] Weiyu Li, Rui Chen, Xuelin Chen, and Ping Tan. Sweetdreamer: Aligning geometric priors in 2d diffusion for consistent text-to-3d. *arXiv preprint arXiv:2310.02596*, 2023.
- [7] Jingxiang Sun, Bo Zhang, Ruizhi Shao, Lizhen Wang, Wen Liu, Zhenda Xie, and Yebin Liu. Dreamcraft3d: Hierarchical 3d generation with bootstrapped diffusion prior. *arXiv preprint arXiv:2310.16818*, 2023.
- [8] Minda Zhao, Chaoyi Zhao, Xinyue Liang, Lincheng Li, Zeng Zhao, Zhipeng Hu, Changjie Fan, and Xin Yu. Efficientdreamer: High-fidelity and robust 3d creation via orthogonal-view diffusion prior. *arXiv preprint arXiv:2308.13223*, 2023.
- [9] Yichun Shi, Peng Wang, Jianglong Ye, Mai Long, Kejie Li, and Xiao Yang. Mvdream: Multi-view diffusion for 3d generation. *arXiv preprint arXiv:2308.16512*, 2023.
- [10] Zilong Chen, Feng Wang, and Huaping Liu. Text-to-3d using gaussian splatting. *arXiv preprint arXiv:2309.16585*, 2023.
- [11] Jiaxiang Tang, Jiawei Ren, Hang Zhou, Ziwei Liu, and Gang Zeng. Dreamgaussian: Generative gaussian splatting for efficient 3d content creation. *arXiv preprint arXiv:2309.16653*, 2023.
- [12] Yixun Liang, Xin Yang, Jiantao Lin, Haodong Li, Xiaogang Xu, and Yingcong Chen. Luciddreamer: Towards high-fidelity text-to-3d generation via interval score matching, 2023.
- [13] Jiaxiang Tang, Zhaoxi Chen, Xiaokang Chen, Tengfei Wang, Gang Zeng, and Ziwei Liu. Lgm: Large multi-view gaussian model for high-resolution 3d content creation. *arXiv preprint arXiv:2402.05054*, 2024.
- [14] Zi-Xin Zou, Zhipeng Yu, Yuan-Chen Guo, Yangguang Li, Ding Liang, Yan-Pei Cao, and Song-Hai Zhang. Triplane meets gaussian splatting: Fast and generalizable single-view 3d reconstruction with transformers. *arXiv preprint arXiv:2312.09147*, 2023.
- [15] Heewoo Jun and Alex Nichol. Shap-e: Generating conditional 3d implicit functions. *arXiv preprint arXiv:2305.02463*, 2023.
- [16] Shoukang Hu, Fangzhou Hong, Tao Hu, Liang Pan, Haiyi Mei, Weiye Xiao, Lei Yang, and Ziwei Liu. Humanliff: Layer-wise 3d human generation with diffusion model. *arXiv preprint arXiv:2308.09712*, 2023.

- [17] Jiatao Gu, Alex Trevithick, Kai-En Lin, Joshua M Susskind, Christian Theobalt, Lingjie Liu, and Ravi Ramamoorthi. Nerfdiff: Single-image view synthesis with nerf-guided distillation from 3d-aware diffusion. In *ICML*, pages 11808–11826. PMLR, 2023.
- [18] Gang Li, Heliang Zheng, Chaoyue Wang, Chang Li, Changwen Zheng, and Dacheng Tao. 3ddesigner: Towards photorealistic 3d object generation and editing with text-guided diffusion models. *arXiv preprint arXiv:2211.14108*, 2022.
- [19] Chen-Hsuan Lin, Jun Gao, Luming Tang, Towaki Takikawa, Xiaohui Zeng, Xun Huang, Karsten Kreis, Sanja Fidler, Ming-Yu Liu, and Tsung-Yi Lin. Magic3d: High-resolution text-to-3d content creation. In *CVPR*, pages 300–309, 2023.
- [20] Aditya Sanghi, Hang Chu, Joseph G Lambourne, Ye Wang, Chin-Yi Cheng, Marco Fumero, and Kamal Rahimi Malekshan. Clip-forge: Towards zero-shot text-to-shape generation. In *CVPR*, pages 18603–18613, 2022.
- [21] Ajay Jain, Ben Mildenhall, Jonathan T Barron, Pieter Abbeel, and Ben Poole. Zero-shot text-guided object generation with dream fields. In *CVPR*, pages 867–876, 2022.
- [22] Oscar Michel, Roi Bar-On, Richard Liu, Sagie Benaim, and Rana Hanocka. Text2mesh: Text-driven neural stylization for meshes. In *CVPR*, pages 13492–13502, 2022.
- [23] Jiabao Lei, Yabin Zhang, Kui Jia, et al. Tango: Text-driven photorealistic and robust 3d stylization via lighting decomposition. *NeurIPS*, 35:30923–30936, 2022.
- [24] Nasir Mohammad Khalid, Tianhao Xie, Eugene Belilovsky, and Tiberiu Popa. Clip-mesh: Generating textured meshes from text using pretrained image-text models. In *SIGGRAPH Asia 2022 conference papers*, pages 1–8, 2022.
- [25] Can Wang, Menglei Chai, Mingming He, Dongdong Chen, and Jing Liao. Clip-nerf: Text-and-image driven manipulation of neural radiance fields. In *CVPR*, pages 3835–3844, 2022.
- [26] Jiale Xu, Xintao Wang, Weihao Cheng, Yan-Pei Cao, Ying Shan, Xiaohu Qie, and Shenghua Gao. Dream3d: Zero-shot text-to-3d synthesis using 3d shape prior and text-to-image diffusion models. In *CVPR*, pages 20908–20918, 2023.
- [27] Fangzhou Hong, Mingyuan Zhang, Liang Pan, Zhongang Cai, Lei Yang, and Ziwei Liu. Avatarclip: Zero-shot text-driven generation and animation of 3d avatars. *arXiv preprint arXiv:2205.08535*, 2022.
- [28] Alec Radford, Jong Wook Kim, Chris Hallacy, Aditya Ramesh, Gabriel Goh, Sandhini Agarwal, Girish Sastry, Amanda Askell, Pamela Mishkin, Jack Clark, et al. Learning transferable visual models from natural language supervision. In *ICML*, pages 8748–8763. PMLR, 2021.
- [29] Haochen Wang, Xiaodan Du, Jiahao Li, Raymond A Yeh, and Greg Shakhnarovich. Score jacobian chaining: Lifting pretrained 2d diffusion models for 3d generation. In *CVPR*, pages 12619–12629, 2023.
- [30] Mohammadreza Armandpour, Huangjie Zheng, Ali Sadeghian, Amir Sadeghian, and Mingyuan Zhou. Re-imagine the negative prompt algorithm: Transform 2d diffusion into 3d, alleviate janus problem and beyond. *arXiv preprint arXiv:2304.04968*, 2023.
- [31] Tianchang Shen, Jun Gao, Kangxue Yin, Ming-Yu Liu, and Sanja Fidler. Deep marching tetrahedra: a hybrid representation for high-resolution 3d shape synthesis. *NeurIPS*, 34:6087–6101, 2021.
- [32] Yimin Luo, Qinyu Yang, Yuheng Fan, Haikun Qi, and Menghan Xia. Measurement guidance in diffusion models: Insight from medical image synthesis. *IEEE Transactions on Pattern Analysis and Machine Intelligence*, 2024.
- [33] Lianghui Zhu, Zilong Huang, Bencheng Liao, Jun Hao Liew, Hanshu Yan, Jiashi Feng, and Xinggang Wang. Dig: Scalable and efficient diffusion models with gated linear attention. *arXiv:2405.18428*, 2024.
- [34] Junshu Tang, Tengfei Wang, Bo Zhang, Ting Zhang, Ran Yi, Lizhuang Ma, and Dong Chen. Make-it-3d: High-fidelity 3d creation from a single image with diffusion prior. *arXiv preprint arXiv:2303.14184*, 2023.
- [35] Minghua Liu, Chao Xu, Haian Jin, Linghao Chen, Zexiang Xu, Hao Su, et al. One-2-3-45: Any single image to 3d mesh in 45 seconds without per-shape optimization. *arXiv preprint arXiv:2306.16928*, 2023.
- [36] Ruoshi Liu, Rundi Wu, Basile Van Hoorick, Pavel Tokmakov, Sergey Zakharov, and Carl Vondrick. Zero-1-to-3: Zero-shot one image to 3d object. *arXiv preprint arXiv:2303.11328*, 2023.

- [37] Guocheng Qian, Jinjie Mai, Abdullah Hamdi, Jian Ren, Aliaksandr Siarohin, Bing Li, Hsin-Ying Lee, Ivan Skorokhodov, Peter Wonka, Sergey Tulyakov, et al. Magic123: One image to high-quality 3d object generation using both 2d and 3d diffusion priors. *arXiv preprint arXiv:2306.17843*, 2023.
- [38] Ruoxi Shi, Hansheng Chen, Zhuoyang Zhang, Minghua Liu, Chao Xu, Xinyue Wei, Linghao Chen, Chong Zeng, and Hao Su. Zero123++: a single image to consistent multi-view diffusion base model. *arXiv preprint arXiv:2310.15110*, 2023.
- [39] Yukang Lin, Haonan Han, Chaoqun Gong, Zunnan Xu, Yachao Zhang, and Xiu Li. Consistent123: One image to highly consistent 3d asset using case-aware diffusion priors. *arXiv preprint arXiv:2309.17261*, 2023.
- [40] Yukai Shi, Jianan Wang, He Cao, Boshi Tang, Xianbiao Qi, Tianyu Yang, Yukun Huang, Shilong Liu, Lei Zhang, and Heung-Yeung Shum. Toss: High-quality text-guided novel view synthesis from a single image. *arXiv preprint arXiv:2310.10644*, 2023.
- [41] Kyle Sargent, Zizhang Li, Tanmay Shah, Charles Herrmann, Hong-Xing Yu, Yunzhi Zhang, Eric Ryan Chan, Dmitry Lagun, Li Fei-Fei, Deqing Sun, et al. Zeronvs: Zero-shot 360-degree view synthesis from a single real image. *arXiv preprint arXiv:2310.17994*, 2023.
- [42] Yuan Liu, Cheng Lin, Zijiao Zeng, Xiaoxiao Long, Lingjie Liu, Taku Komura, and Wenping Wang. Syncdreamer: Generating multiview-consistent images from a single-view image. *arXiv preprint arXiv:2309.03453*, 2023.
- [43] Xiaoxiao Long, Yuan-Chen Guo, Cheng Lin, Yuan Liu, Zhiyang Dou, Lingjie Liu, Yuexin Ma, Song-Hai Zhang, Marc Habermann, Christian Theobalt, et al. Wonder3d: Single image to 3d using cross-domain diffusion. *arXiv preprint arXiv:2310.15008*, 2023.
- [44] Jianglong Ye, Peng Wang, Kejie Li, Yichun Shi, and Heng Wang. Consistent-1-to-3: Consistent image to 3d view synthesis via geometry-aware diffusion models. *arXiv preprint arXiv:2310.03020*, 2023.
- [45] Zhenzhen Weng, Zeyu Wang, and Serena Yeung. Zeroavatar: Zero-shot 3d avatar generation from a single image. *arXiv preprint arXiv:2305.16411*, 2023.
- [46] Jiayu Yang, Ziang Cheng, Yunfei Duan, Pan Ji, and Hongdong Li. Consistnet: Enforcing 3d consistency for multi-view images diffusion. *arXiv preprint arXiv:2310.10343*, 2023.
- [47] Haohan Weng, Tianyu Yang, Jianan Wang, Yu Li, Tong Zhang, CL Chen, and Lei Zhang. Consistent123: Improve consistency for one image to 3d object synthesis. *arXiv preprint arXiv:2310.08092*, 2023.
- [48] Alex Nichol, Heewoo Jun, Pratul Dhariwal, Pamela Mishkin, and Mark Chen. Point-e: A system for generating 3d point clouds from complex prompts. *arXiv preprint arXiv:2212.08751*, 2022.
- [49] Ankit Gupta, Wenhan Xiong, Yixin Nie, Ian Jones, and Barlas Oğuz. 3dgen: Triplane latent diffusion for textured mesh generation. *arXiv preprint arXiv:2303.05371*, 2023.
- [50] Jun Gao, Tianchang Shen, Zian Wang, Wenzheng Chen, Kangxue Yin, Daiqing Li, Or Litany, Zan Gojcic, and Sanja Fidler. Get3d: A generative model of high quality 3d textured shapes learned from images. *NeurIPS*, 35:31841–31854, 2022.
- [51] Yicong Hong, Kai Zhang, Jiuxiang Gu, Sai Bi, Yang Zhou, Difan Liu, Feng Liu, Kalyan Sunkavalli, Trung Bui, and Hao Tan. Lrm: Large reconstruction model for single image to 3d. *arXiv preprint arXiv:2311.04400*, 2023.
- [52] Jiahao Li, Hao Tan, Kai Zhang, Zexiang Xu, Fujun Luan, Yinghao Xu, Yicong Hong, Kalyan Sunkavalli, Greg Shakhnarovich, and Sai Bi. Instant3d: Fast text-to-3d with sparse-view generation and large reconstruction model. *arXiv preprint arXiv:2311.06214*, 2023.
- [53] QiuHong Shen, Xuanyu Yi, Zike Wu, Pan Zhou, Hanwang Zhang, Shuicheng Yan, and Xinchao Wang. Gamba: Marry gaussian splatting with mamba for single view 3d reconstruction. *arXiv preprint arXiv:2403.18795*, 2024.
- [54] Ben Mildenhall, Pratul P Srinivasan, Matthew Tancik, Jonathan T Barron, Ravi Ramamoorthi, and Ren Ng. Nerf: Representing scenes as neural radiance fields for view synthesis. In *ECCV*, pages 405–421, 2020.
- [55] Thomas Müller, Alex Evans, Christoph Schied, and Alexander Keller. Instant neural graphics primitives with a multiresolution hash encoding. *ACM Trans. Graph.*, 41(4):102:1–102:15, July 2022.

- [56] Anpei Chen, Zexiang Xu, Andreas Geiger, Jingyi Yu, and Hao Su. Tensorf: Tensorial radiance fields. In *European Conference on Computer Vision*, pages 333–350. Springer, 2022.
- [57] Cheng Sun, Min Sun, and Hwann-Tzong Chen. Improved direct voxel grid optimization for radiance fields reconstruction. *arXiv preprint arXiv:2206.05085*, 2022.
- [58] Cheng Sun, Min Sun, and Hwann-Tzong Chen. Direct voxel grid optimization: Super-fast convergence for radiance fields reconstruction. In *Proceedings of the IEEE/CVF Conference on Computer Vision and Pattern Recognition*, pages 5459–5469, 2022.
- [59] Sara Fridovich-Keil, Alex Yu, Matthew Tancik, Qinhong Chen, Benjamin Recht, and Angjoo Kanazawa. Plenoxels: Radiance fields without neural networks. In *Proceedings of the IEEE/CVF Conference on Computer Vision and Pattern Recognition*, pages 5501–5510, 2022.
- [60] Guikun Chen and Wenguan Wang. A survey on 3d gaussian splatting. *arXiv preprint arXiv:2401.03890*, 2024.
- [61] Jonathan T Barron, Ben Mildenhall, Matthew Tancik, Peter Hedman, Ricardo Martin-Brualla, and Pratul P Srinivasan. Mip-nerf: A multiscale representation for anti-aliasing neural radiance fields. In *ICCV*, pages 5855–5864, 2021.
- [62] Jonathan T Barron, Ben Mildenhall, Dor Verbin, Pratul P Srinivasan, and Peter Hedman. Mip-nerf 360: Unbounded anti-aliased neural radiance fields. In *Proceedings of the IEEE/CVF Conference on Computer Vision and Pattern Recognition*, pages 5470–5479, 2022.
- [63] Binbin Huang, Zehao Yu, Anpei Chen, Andreas Geiger, and Shenghua Gao. 2d gaussian splatting for geometrically accurate radiance fields. *arXiv preprint arXiv:2403.17888*, 2024.
- [64] Antoine Guédon and Vincent Lepetit. Sugar: Surface-aligned gaussian splatting for efficient 3d mesh reconstruction and high-quality mesh rendering. *arXiv preprint arXiv:2311.12775*, 2023.
- [65] Bardienus P Duisterhof, Zhao Mandi, Yunchao Yao, Jia-Wei Liu, Mike Zheng Shou, Shuran Song, and Jeffrey Ichnowski. Md-splatting: Learning metric deformation from 4d gaussians in highly deformable scenes. *arXiv preprint arXiv:2312.00583*, 2023.
- [66] David Svitov, Pietro Morerio, Lourdes Agapito, and Alessio Del Bue. Haha: Highly articulated gaussian human avatars with textured mesh prior. *arXiv preprint arXiv:2404.01053*, 2024.
- [67] Zhijing Shao, Zhaolong Wang, Zhuang Li, Duotun Wang, Xiangru Lin, Yu Zhang, Mingming Fan, and Zeyu Wang. Splattingavatar: Realistic real-time human avatars with mesh-embedded gaussian splatting. *arXiv preprint arXiv:2403.05087*, 2024.
- [68] Jing Wen, Xiaoming Zhao, Zhongzheng Ren, Alexander G Schwing, and Shenlong Wang. Gomavatar: Efficient animatable human modeling from monocular video using gaussians-on-mesh. *arXiv preprint arXiv:2404.07991*, 2024.
- [69] Tianyi Xie, Zeshun Zong, Yuxing Qiu, Xuan Li, Yutao Feng, Yin Yang, and Chenfanfu Jiang. Physgaussian: Physics-integrated 3d gaussians for generative dynamics. *arXiv preprint arXiv:2311.12198*, 2023.
- [70] Ying Jiang, Chang Yu, Tianyi Xie, Xuan Li, Yutao Feng, Huamin Wang, Minchen Li, Henry Lau, Feng Gao, Yin Yang, et al. Vr-gs: A physical dynamics-aware interactive gaussian splatting system in virtual reality. *arXiv preprint arXiv:2401.16663*, 2024.
- [71] Zhiqi Li, Yiming Chen, Lingzhe Zhao, and Peidong Liu. Controllable text-to-3d generation via surface-aligned gaussian splatting. *arXiv preprint arXiv:2403.09981*, 2024.
- [72] Jiaming Song, Chenlin Meng, and Stefano Ermon. Denoising diffusion implicit models. *arXiv preprint arXiv:2010.02502*, 2020.
- [73] Michael Kazhdan, Matthew Bolitho, and Hugues Hoppe. Poisson surface reconstruction. In *Proceedings of the fourth Eurographics symposium on Geometry processing*, 2006.
- [74] Adam Paszke, Sam Gross, Francisco Massa, Adam Lerer, James Bradbury, Gregory Chanan, Trevor Killeen, Zeming Lin, Natalia Gimelshein, Luca Antiga, et al. Pytorch: An imperative style, high-performance deep learning library. *NeurIPS*, 32, 2019.
- [75] Diederik P Kingma and Jimmy Ba. Adam: A method for stochastic optimization. *arXiv preprint arXiv:1412.6980*, 2014.

- [76] Robin Rombach, Andreas Blattmann, Dominik Lorenz, Patrick Esser, and Björn Ommer. High-resolution image synthesis with latent diffusion models. In *CVPR*, pages 10684–10695, 2022.
- [77] Matt Deitke, Dustin Schwenk, Jordi Salvador, Luca Weihs, Oscar Michel, Eli VanderBilt, Ludwig Schmidt, Kiana Ehsani, Aniruddha Kembhavi, and Ali Farhadi. Objaverse: A universe of annotated 3d objects. In *CVPR*, pages 13142–13153, 2023.
- [78] Tiange Luo, Chris Rockwell, Honglak Lee, and Justin Johnson. Scalable 3d captioning with pretrained models. *arXiv preprint arXiv:2306.07279*, 2023.